

Identification of Common Ferroptosis Signature Genes in Hepatocellular Carcinoma and Renal Clear Cell Carcinoma: Implications for Diagnosis and Prognosis

Xusheng Zhang^{1#}, Hongcai Zhou^{1#}, Peng Wei¹, Weihu Ma¹, Bendong Chen^{2*}

[#]These authors contributed equally to this work and share first authorship

¹Ningxia Medical University, Yinchuan 750004, China

²General Hospital of Ningxia Medical University, Yinchuan 750004, China

Research Article

Received: 01-Apr-2024,
Manuscript No. JMB-24-131109;
Editor assigned: 03-Apr-2024,
PreQC No. JMB-24-131109(PQ);
Reviewed: 17-Apr-2024,
QC No. JMB-24-131109;
Revised: 24-Apr-2024,
Manuscript No. JMB-24-131109(R);
Published: 01-May-2024,
DOI: 10.4172/2320-3528.13.1.002

***For Correspondence:**

Bendong Chen, General Hospital of
Ningxia Medical University, Yinchuan
750004, China

E-mail: chenbendong@nxmu.edu.cn

Citation: Zhang X, et al. Identification
of Common Ferroptosis Signature
Genes in Hepatocellular Carcinoma
and Renal Clear Cell Carcinoma:
Implications for Diagnosis and
Prognosis. J Microbiol Biotechnol.
2024;13:002

Copyright: ©2024 Zhang X, et al. This
is an open-access article distributed
under the terms of the Creative
Commons Attribution License, which
permits unrestricted use, distribution,
and reproduction in any medium,
provided the original author and
source are credited.

ABSTRACT

Objective: To investigate the biological significance of ferroptosis in hepatocellular carcinoma and renal clear cell carcinoma based on their disease commonality.

Methods: Based on the mRNA-seq data and matched clinical data of the two cancers in the GEO (Gene Expression Omnibus) database and TCGA (The Cancer Genome Atlas) database, we used R package and part of online analysis tools to find the differentially expressed ferroptosis genes in the two cancers, and then used LASSO (Least Absolute Shrinkage and Selection Operator) regression analysis to further screen the ferroptosis signature genes in the two cancers, explored their functional characteristics and clinical significance in the two cancers based on the expression of the ferroptosis signature genes.

Results: Four ferroptosis genes, *G6PD*, *NRAS*, *CDCA3* and *NDRG1* were significantly upregulated in hepatocellular carcinoma and renal clear cell carcinoma showed good diagnostic efficacy for both cancers, and were significantly associated with patient survival prognosis. The risk model based on the four characteristic genes showed good predictive efficacy and has potential clinical application, upregulation of *NRAS* expression may contribute to the pathogenesis and progression of cancer through activation of MAPK/ERK signalling pathway.

Conclusion: *G6PD*, *NRAS*, *CDCA3*, and *NDRG1* are common ferroptosis signature genes for hepatocellular carcinoma and renal clear cell carcinoma, which have good diagnostic and prognostic predictive efficacy for both cancers, upregulation of *NRAS* expression may contribute to the pathogenesis and progression of two cancer through activation of MAPK/ERK signaling pathway.

Keywords: Ferroptosis genes; Hepatocellular carcinoma; Pathogenesis; Progression; Clinical application

INTRODUCTION

Hepatocellular Carcinoma (HCC) is the most common primary liver cancer, accounting for approximately 75% to 85% of liver cancers [1]. According to the latest statistics, HCC ranks sixth among all cancers and is also the third most lethal cancer, while domestic statistics show that primary liver cancer ranks as the fourth most common malignant tumor and the second most lethal cause of tumor, seriously threatening human life and health [2,3]. Renal Cell Carcinoma (RCC) originates from the urinary tubular epithelial system of the renal parenchyma, the number of new cases and deaths of renal tumors in China were about 431,288 and 179,368 respectively, in 2020. The early clinical manifestations of RCC are insidious, and about 30% of patients have different degrees of metastasis at the time of consultation. While Clear Cell Renal Cell Carcinoma (CCRCC) is the most predominant subtype of renal cancer, accounting for about 80% of RCC, in metastatic Renal Cell Carcinoma (mRCC), its pathological type is almost always CCRCC [3].

Both HCC and CCRCC are cancers of substantial organs, both of which are insidious in their onset, and metastatic cancers can occur between the two diseases clinically. Furthermore, there are similarities in the treatment of these two types of cancers, such as sorafenib, which was first used in kidney cancer, is now widely used in the treatment of HCC, lenvatinib is also approved for unresectable or advanced HCC and advanced RCC, etc; [3,4] suggesting the presence of identical immune targets expression in both cancers. Ferroptosis is a newly proposed form of cell death

caused by iron-dependent lipid peroxidation and massive accumulation of reactive oxygen (ROS) radicals, following apoptosis, autophagy, pyroptosis, necrosis, and is widely present in the metabolic process of tumors. It has been shown that induction of ferroptosis can inhibit tumor cell proliferation, reverse radiotherapy resistance, and provide new ideas for tumor treatment. Based on these commonalities between the two types of cancers and the extensive involvement of ferroptosis in the metabolic processes of HCC and CCRCC, this study combined the mRNA-seq data from the GEO database and TCGA database to explore the common ferroptosis signature genes in the two cancers in depth and in multiple dimensions using bioinformatic analysis techniques, with the aim of providing a certain research basis for relevant studies on the diagnosis and treatment of the two cancers.

MATERIALS AND METHODS

Study subjects

The gene expression profiles related to this study were obtained from the GEO (<https://www.ncbi.nlm.nih.gov/geo/>) database and TCGA ([HTTP://portal.gdc.cancer.gov/](http://portal.gdc.cancer.gov/)) database, and the data of both TCGA and GEO are open without any related interests and infringement disputes, therefore, for this study local ethics committee approval was not required. This study followed the data access policy and publication guidelines of GEO and TCGA.

R-based analysis

This study is based on the GEO database GSE53757 (CCRCC), GSE47197 (HCC) datasets, TCGA database of clear cell carcinoma, TCGA database of hepatocellular carcinoma mRNA-Seq and corresponding clinical data. Differential expression analysis was performed by R "limma" package to obtain ferroptosis genes that were differentially expressed in both cancers, GO and KEGG analysis was performed by R "clusterProfiler" package to explore the biological functions and signaling pathways associated with the intersecting genes ($P < 0.05$ was statistically significant). The intersecting genes were further screened by 'LASSO' regression analysis using the R 'survival'/'caret'/'glmnet'/'survivalROC' packages, and the diagnostic efficacy of the signature genes was analyzed using the 'pROC' package. The impact of signature genes on survival prognosis was analyzed using the R "survminer" package. The unsupervised clustering analysis was performed using the R "ConsensusClusterPlus" package and validated using the "limma" and "ggplot2" packages. The correlation between signature genes and immune checkpoints was also analyzed using the "corrplot" package. The effect of signature genes on the infiltration abundance of tumor immune cells was analyzed using the R "GSVA" package.

VENNY 2.1-based analysis

VENNY 2.1 (<https://bioinfogp.cnb.csic.es/tools/venny/index.html>) is an online protein intersection analysis tool that can accommodate up to four sets of data simultaneously for online analysis. In this study, the online tool from this site was used to take intersections of differentially expressed ferroptosis genes in two cancers.

STRING-based analysis

The protein interaction networks of differentially expressed genes in two cancers were constructed using STRING (Search Tool for the Retrieval of Interacting Genes/Proteins) (string-db.org) database, and a confidence score > 0.4 was considered to be a good correlation. The obtained PPI networks were imported into Cytoscape 3.6.1 software, and their feature clustering modules were filtered using the MCODE clustering plugin.

Statistical analysis

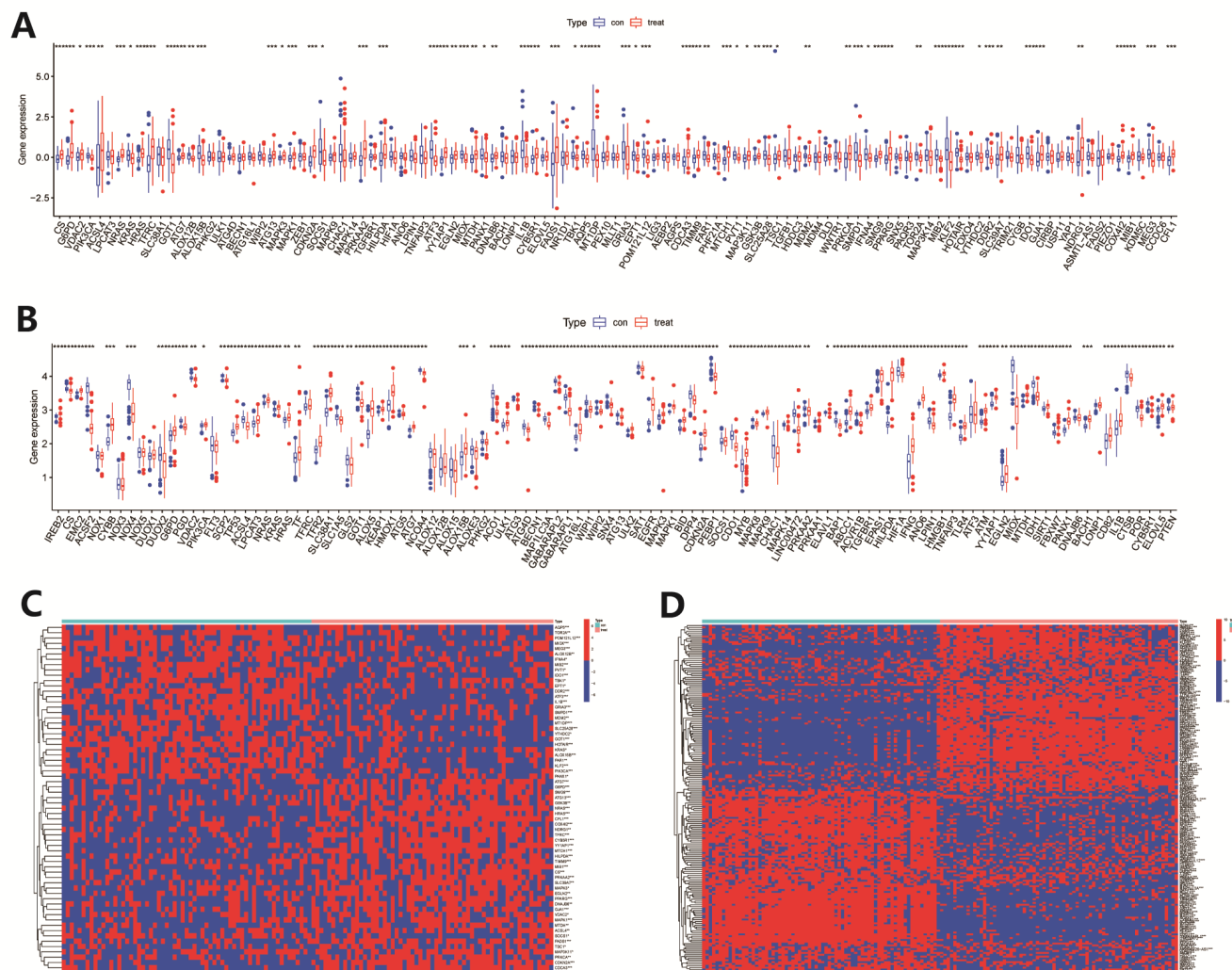
Statistical analysis and plots were performed using R 4.1.1, and measurement data conforming to normal distribution were expressed as mean \pm standard deviation, and Wilcoxon rank sum test was used for comparison between groups; chi-square test was used for comparison between groups of count data. Spearman correlation analysis was used for simple correlation analysis of measurement data not conforming to normal distribution. $p < 0.05$ was statistically significant.

RESULTS

Expression of ferroptosis genes in HCC and CCRCC

In this study, we first analyzed the expression of ferroptosis genes in normal and tumor tissues in the GEO database GSE53757 (renal clear cell carcinoma) and GSE47197 (HCC) datasets, and the results showed that the expression levels of 187 ferroptosis genes in CCRCC differed from those in normal kidney tissues, and 65 ferroptosis genes were differentially expressed in hepatocellular carcinoma compared with normal liver tissues, and box plots and heat maps were further plotted for the differentially expressed ferroptosis genes in the two cancers (Figures 1A and 1B). See supplementary material for complete box plots.

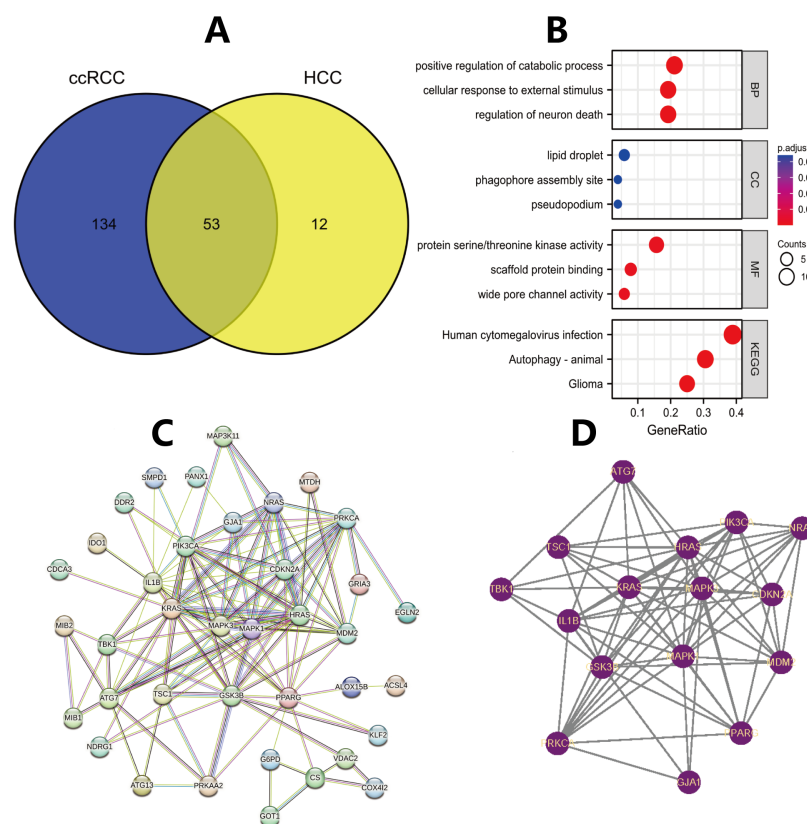
Figure 1. Expression analysis of ferroptosis-related genes in CCRCC versus HCC. (A) Expression of ferroptosis genes in normal tissues versus HCC; (B) Expression of ferroptosis genes in normal tissues versus CCRCC. **Note:** Con; Treat.



GO/KEGG enrichment analysis of intersecting genes and protein interaction network

An online analysis tool VEENY 2.1 was used to intersect 187 differentially expressed ferroptosis genes in RCC and 65 differentially expressed ferroptosis genes in HCC. Then, we found 53 differentially expressed ferroptosis genes in both cancers (Figure 2A). Subsequently, functional and pathway enrichment analysis of these 53 differentially expressed ferroptosis genes showed that they were mainly enriched in the Biological Process (BP): Regulation of neuron death, positive regulation of catabolic process, cellular response to external stimulus. The Cellular Component (CC) is mainly enriched in pseudopodium, lipid droplet, phagophore assembly site, etc. The molecular Function (MF) level is mainly enriched in: Scaffold protein binding, wide pore channel activity, and protein serine/threonine kinase activity. KEGG is mainly involved in human cytomegalovirus infection, autophagy-animal, glioma and other signalling pathways (Figure 2B). Following that, the protein interaction network among these 53 ferroptosis-related genes was analyzed (Figure 2C), and the main modules in the protein interaction network were clustered using the MCODE clustering plugin (Figure 2D).

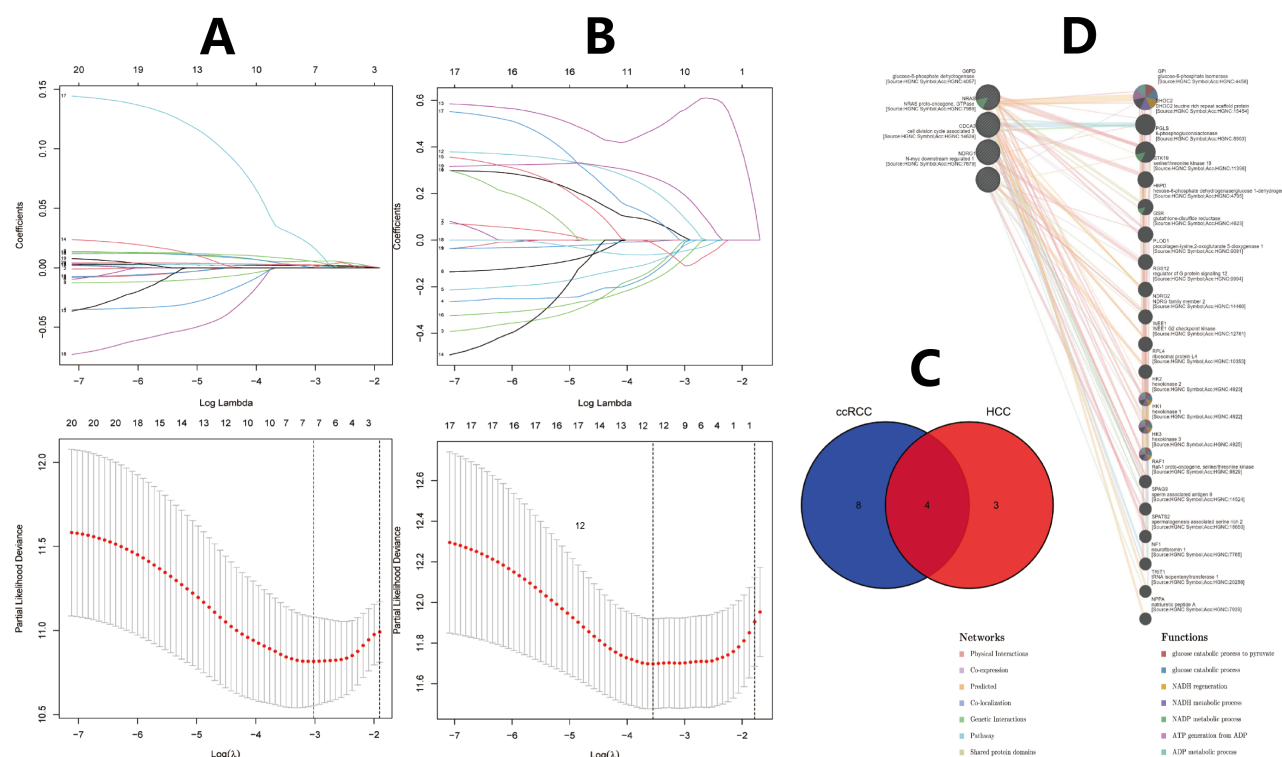
Figure 2. Intersection genes and their GO/KEGG enrichment analysis with protein interaction network. (A) Intersection venn diagram of differentially expressed ferroptosis genes in CCRCC and HCC; (B) GO/KEGG enrichment analysis of intersection genes; (C) Protein interaction network of intersection genes; (D) Major clustering modules in protein interaction network of intersection genes.



Screening of characterization genes

Following this study, LASSO regression analysis was performed separately for the intersecting ferroptosis genes in the two cancers and prognostic models were established ($P < 0.01$, ROC-AUC > 0.7), and the results showed that 7 ferroptosis-related genes were screened for modelling in HCC and 12 genes were screened for modelling in CCRCC ferroptosis related genes were screened for modelling (Figures 3A and 3B). Then, the study took the intersection of the ferroptosis genes used for modelling in HCC and CCRCC, and as a result, four genes, *NRAS/G6PD/CDCA3* and *NDRG1*, were selected in the modelling process of both cancers (Figure 3C) and were identified as common ferroptosis signature genes in both cancers. Subsequently, these associated genes with the co-localization, co-expression, and common biological functions of the four signature genes were explored. The results showed that these genes are mainly involved in the processes of glucose metabolism, NADP and NADH metabolism, ADP metabolism and ATP production (Figure 3D).

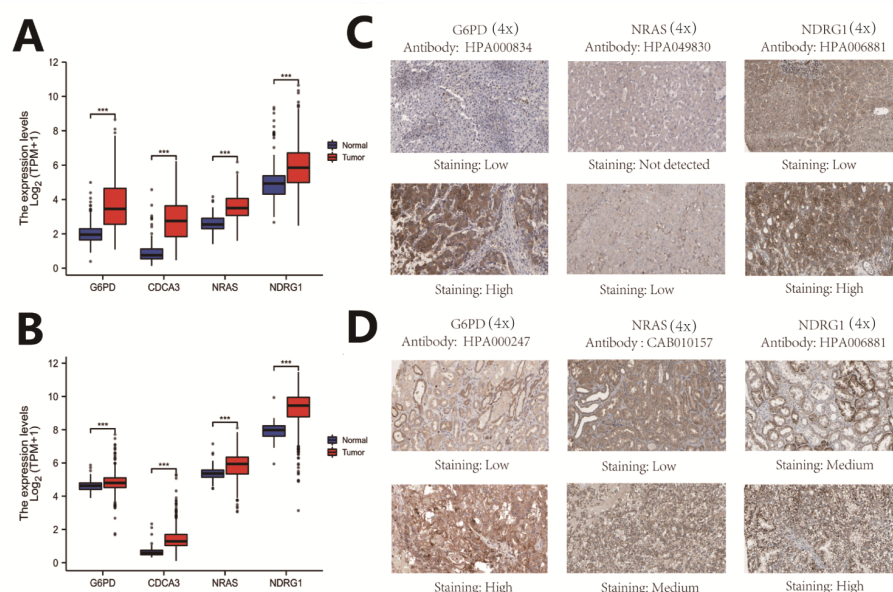
Figure 3. (A-B) Separate LASSO regression analysis of intersecting genes in HCC and CCRCC; (C) Intersection of genes screened by LASSO regression analysis in both cancers was taken to identify the signature genes; (D) Correlation gene analysis of the four signature genes. **Note:** ■ Physical interactions; ■ Co-expression; ■ Predicted; ■ Co-localization; ■ Genetic interactions; ■ Pathway; ■ Shared protein domains; ■ Glucose catabolic process to pyruvate; ■ Glucose catabolic process; ■ NADH regeneration; ■ NADH metabolic process; ■ NADP metabolic process; ■ ATP generation from ADP; ■ ADP metabolic process.



Characteristic genes expression analysis in HCC and CCRCC

After identifying *NRAS/G6PD/CDCA3* and *NDRG1* as characteristic ferroptosis genes in HCC and CCRCC, we further analyzed the expression of the four ferroptosis genes in HCC and CCRCC, and the results showed that the four genes were significantly upregulated in both cancers (Figures 4A and 4B) ($P < 0.001$). To further assess the reliability of the above analysis, we further analyzed the expression of the four ferroptosis signature genes based on the Human Genetic Atlas (HPA), and immunohistochemical staining suggested that *NRAS*, *G6PD* and *NDRG1* showed upregulated expression in both cancers compared with normal tissues (Figures 4C and 4D), while the expression of *CDCA3* immunohistochemical results were not included at this time.

Figure 4. Characteristic gene expression analysis in HCC and CCRCC. (A) *NRAS*, *G6PD*, *CDCA3* and *NDRG1* expression in HCC; (B) *NRAS/G6PD/CDCA3* and *NDRG1* expression in CCRCC; (C) Immunohistochemical results of *NRAS*, *G6PD* and *NDRG1* in HCC; (D) Immunohistochemical results of *NRAS/G6PD* and *NDRG1* in CCRCC. **Note:** ■ Normal; ■ Tumor.



Diagnostic efficacy analysis of the signature genes

After screening out the four signature genes, we explored the diagnostic efficacy of the four signature genes using mRNA-Seq data of HCC and CCRCC in the TCGA database, and the results showed that the ROC-AUCs of the four genes in HCC were 0.863, 0.983, 0.809, and 0.950 (Figure S1A) and in CCRCC were 0.740, 0.905, 0.893, and 0.629 (Figure S1B), respectively. Except for the poor diagnostic efficacy of G6PD in CCRCC, the other three ferroptosis genes showed good diagnostic efficacy for both cancers.

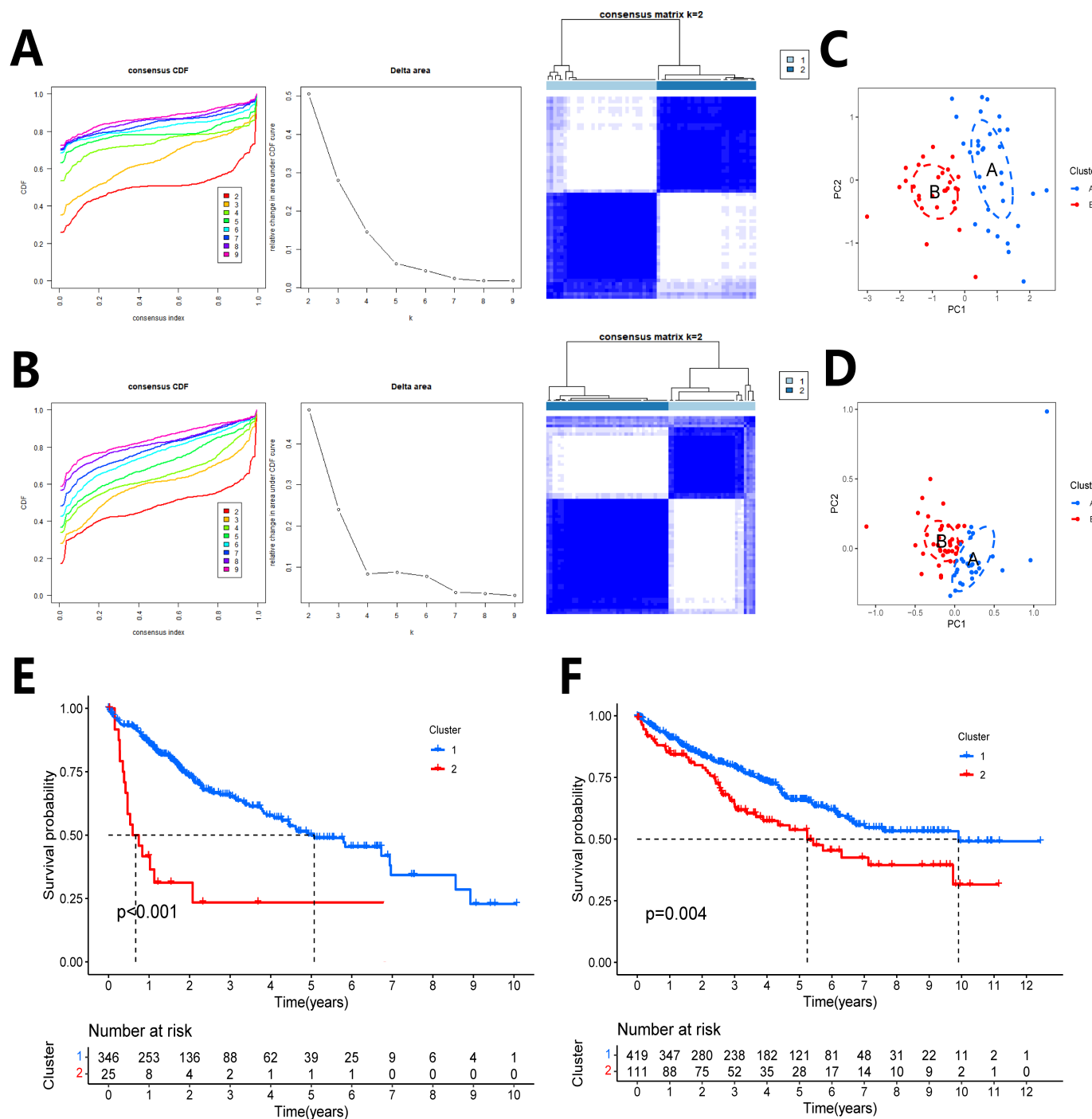
Prognostic analysis of the four ferroptosis signature genes

After determining the diagnostic efficacy of the four signature genes, we further analyzed the prognostic impact of the four genes on survival in two diseases, and the results showed that the four signature genes showed significant prognostic correlation in both diseases ($P < 0.05$), and high expression in HCC was associated with poorer prognosis of patients in both diseases (Figure S2A), while high expression of *NDRG1* and *NRAS* in CCRCC were associated with better survival prognosis of patients, respectively (Figure S2B), suggesting that the role of the two in CCRCC is characterized differently from that in HCC.

Subtype analysis and validation of the results

Based on the expression of the four ferroptosis signature genes in the TCGA database, we performed unsupervised cluster analysis on the samples included in the two cancers separately, and the results showed that the samples were clearly divided into two groups cluster 1 and cluster 2 in both HCC and CCRCC (Figures 5A and 5B). Then, to verify the reliability of the results of the unsupervised cluster analysis, a principal component analysis was performed on the samples, and the results also clearly divided the samples into two subgroups, cluster A and cluster B (Figures 5C and 5D). Finally, we analyzed the survival relationship between the subgroups based on the expression of the four ferroptosis signature genes, and the results showed a significant difference in survival between the two groups in both HCC and CCRCC (Figures 5E and 5F) ($P < 0.005$).

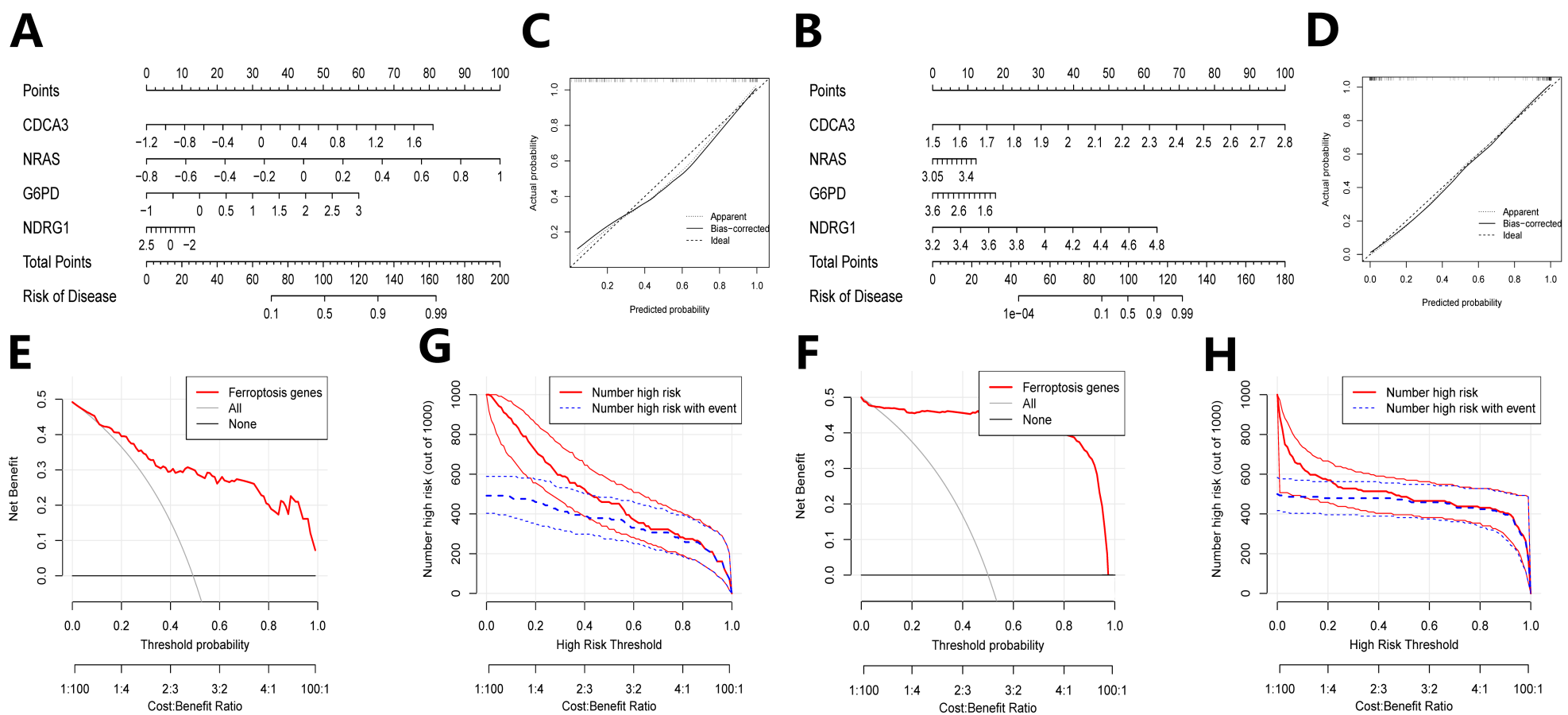
Figure 5. Subtype analysis and validation of the results and validation of the results. (A) Unsupervised cluster analysis for HCC; (B) Unsupervised cluster analysis for CCRCC; (C) Principal component analysis for HCC; (D) Principal component analysis for CCRCC; (E) Survival analysis between subgroups of HCC; (F) Survival analysis between subgroups of CCRCC. **Note:** ■ Consensus matrix 1; ■ Consensus matrix 2; ■ Consensus CDF 2; ■ Consensus CDF 3; ■ Consensus CDF 4; ■ Consensus CDF 5; ■ Consensus CDF 6; ■ Consensus CDF 7; ■ Consensus CDF 8; ■ Consensus CDF 9; → Cluster A; → Cluster B; → Cluster 1; → Cluster 2.



Construction and validation of risk nomogram model

After determining the diagnostic and prognostic efficacy of the four signature genes, we further constructed the nomogram risk prediction models based on the expression of the four signature genes (Figures 6A and 6B), and then evaluated the predictive efficacy of the nomogram by plotting calibration curves, which showed a good fit (Figures 6C and 6D), suggesting that the predictive efficacy of the nomogram was effective. We then analyzed the clinical performance of the nomogram model, and the decision curves (DCA) showed a good net clinical benefit for patients in both models (Figures 6E and 6F). We also plotted the clinical impact curve, and saw that the model predicted a good true positive prediction rate in our cases, further validating the clinical performance of the line plot model.

Figure 6. Construction and validation of risk nomogram model. (A) Nomogram of HCC; (B) Nomogram of CCRCC; (C) Calibration curves of HCC; (D) Calibration curves of CCRCC; (E) Decision curves (DCA) of HCC.;(F) Decision curves (DCA) of CCRCC; (G) Clinical impact curve for HCC; (H) Clinical impact curve for CCRCC. **Note:** Apparent; — Bias-corrected; ---- Ideal; — Ferropoptosis genes; — All; — None; — Number high risk; Number high risk with event.



Correlation analysis of signature genes and immune targets in two cancers

In this study, we also explored the relationship between four ferroptosis genes and immune checkpoint-related genes in two cancers using the "Limma", "corrplot" R package as shown in Figure S3A. In HCC, G6PD was associated with *CD276*, *TNFSF18*, *TIGIT*, *HAVCR2*, *CD70*, *TNFSF4*, *CD80*, *LAIR1*, *PDCD1* (PD-L1), *ICOS*, *TNFSF9*, *CD86*, *CD44*, *TNFSF14*, *LGALS9*, *TNFSF8*, *CTLA4* and *CD274* (PD-1), and showed good positive correlations ($r > 0.25$). NRAS also showed a good positive trend ($r > 0.25$) with immune checkpoints such as *CD276*, *CD28*, *HAVCR2*, *TNFSF4*, *CD200*, *CD80*, *LAIR1*, *TNFSF18*, *CD86*, *CD200R1*, *NRP1*, *CD274* (PD-1) and *VTCN1*. NDRG1 showed a significant positive trend ($r > 0.25$) with *CD276*, *TNFSF18*, *HAVCR2*, *TNFSF4*, *TNFSF15*, *LAIR1*, *TNFSF8*, *CD86*, *HHLA2*, *LGALS9* and *NRP1* ($r > 0.25$). CDCA3 showed positive correlation with immune checkpoints such as *CD276*, *TNFSF18*, *TIGIT*, *HAVCR2*, *CD70*, *TNFSF4*, *TNFRSF4*, *LAIR1*, *PDCD1* (PD-L1), *ICOS*, *CD86*, *TNFRSF14*, *LGALS9*, *LAG3*, *TNFRSF8*, *CTLA4* ($r > 0.3$). In contrast, in CCRCC, G6PD showed a significant positive correlation mainly with immune checkpoints *CD276*, *PDCD1* (PD-L1), *LGALS9*, *TMIGD2*, *TNFRSF8*, *TNFRSF18*, *CD44* ($r \geq 0.3$). NRAS showed a positive correlation with immune checkpoints *CD200*, *NRP1*, *TNFSF4*, *CD28*, *CD200R1*, *HAVCR2*, *PDCD1LG2*, *TNFSF18*, *CD86* ($r \geq 0.3$). NDRG1 was positively correlated with *CD200*, *TNFRSF4*, *HAVCR2*, *ADORA2A*, *IDO1*, *HHLA2*, *CD70*, *TNFSF9* and other immune targets ($r > 0.25$). CDCA3 was correlated with *TNFSF4*, *LAG3*, *CTLA4*, *PDCD1*, *CD276*, *LGALS9*, *TNFSF14*, *TMIGD2*, *TNFRSF8*, *CD27*, *TNFRSF18*, *TNFRSF25*, *TIGIT*, *CD44*, *TNFRSF9*, and showed significant positive correlation with them ($r \geq 0.3$) (Figure S3B).

Correlation analysis of signature genes with tumor immune cell infiltration

At the end of the study, we analyzed the relationship between each of the four ferroptosis signature genes and the infiltration of immune cells in the two cancers, and the results showed that in HCC (Figures S4A-S4D) CDCA3 was positively correlated with the infiltration of immune cells such as Th2 cells, TFH, NK CD56 bright cells, T helper cells, and negatively correlated with the infiltration of neutrophils, DCs, Th17 cells and other immune cells ($|r| > 0.2$) ($P < 0.001$). G6PD mainly showed a significant positive correlation with the infiltration of immune cells such as Th2 cells, NK CD56 bright cells, macrophages, T helper cells, TFH, aDC, Th1 cells, and a negative correlation with the infiltration of immune cells such as Th17 cells ($|r| > 0.2$) ($P < 0.001$). NRAS was positively correlated with immune cells such as Th2 cells, T helper cells, Tcm, and negatively

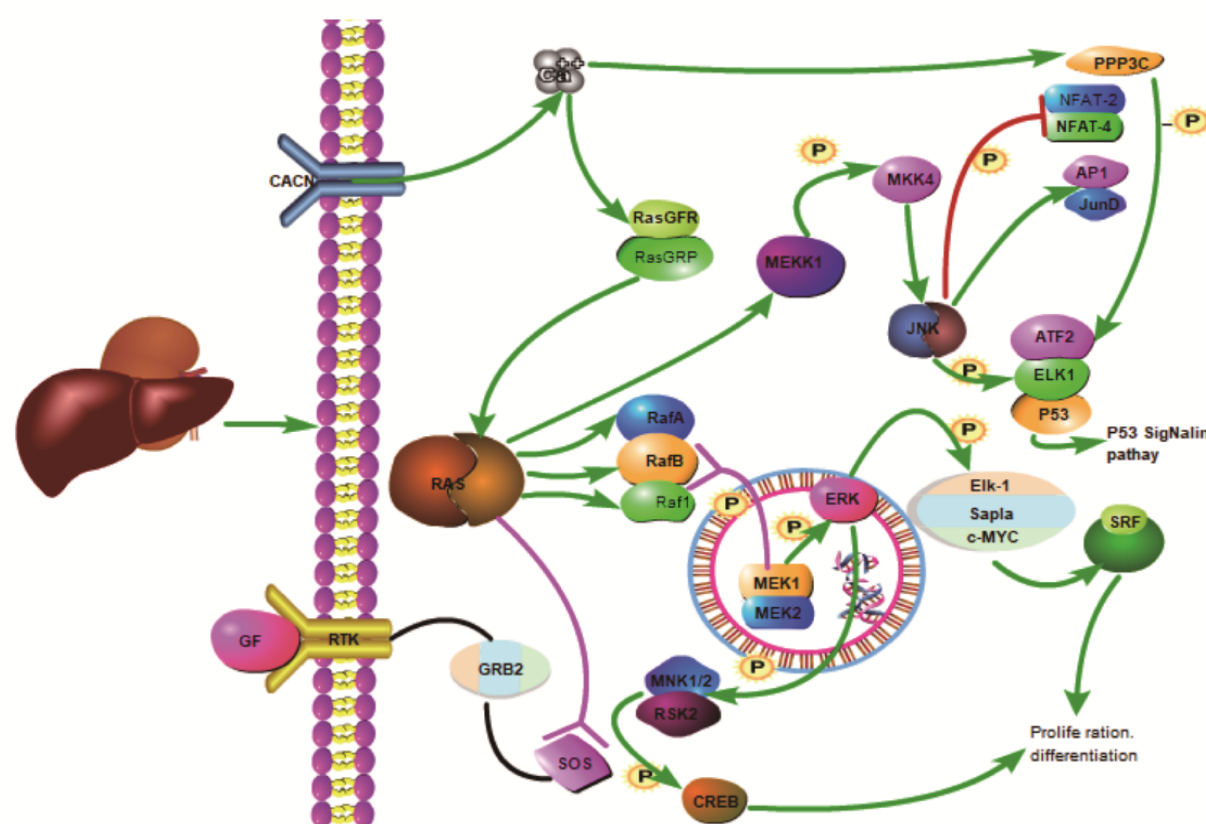
correlated with immune cells such as pDC, cytotoxic cells, CD8 T cells ($|r| > 0.2$) ($P < 0.001$). *NDRG1* was positively correlated with immune cells such as Th2 cells, NK CD56 bright cells and TFH, and negatively correlated with infiltration of immune cells such as pDC, DC, cytotoxic cells ($|r| > 0.2$) ($P < 0.001$). While in CCRCC (Figures S4E-S4H), *CDCA3* was mainly positively correlated with the infiltration of immune cells such as Th2 cells, TReg, Th1 cells, NK CD56 bright cells, and negatively correlated with immune cells such as Th17 cells, mast cells, pDC ($|r| > 0.2$) ($P < 0.001$). *G6PD* was mainly positively correlated with immune cells such as Th2 cells, TReg, DC, NK CD56 bright cells, iDC, B cells, macrophages, Th1 cells ($|r| > 0.2$) ($P < 0.001$). *NRAS* was mainly correlated with Tcm, neutrophils, T helper *NRAS* was positively correlated with immune cells such as Tcm, neutrophils, T helper cells, eosinophils, Tem, Tgd, Th2 cells, mast cells, macrophages and negatively correlated with the infiltration level of NK CD56 bright cells ($|r| > 0.2$) ($P < 0.001$). *NDRG1* was mainly correlated with NK CD56 dim cells, NK cells, eosinophils, Th17 cells, neutrophils, and were positively associated with the level of infiltration of immune cells ($|r| > 0.2$) ($P < 0.001$).

Signaling pathway analysis

At the end of the study we also explored the involvement of four ferroptosis genes in the signaling pathway using the KEGG PATHWAY Database (<https://www.kegg.jp/kegg/kegg2.html>) database. It was found that *NRAS* is involved in MAPK signaling pathway regulation and *NRAS* expression can sequentially activate the MAPK/ERK signaling pathway (Figure 7), which has a strong association with cancer development by promoting cell proliferation and differentiation processes and further influencing the cell cycle. Among the pathways involved in the metabolic process of HCC, we also found that MAPK/ERK signaling pathway is involved and is one of the major pathways, suggesting that MAPK/ERK signaling pathway plays a very important role in the whole disease process of HCC.

Figure 7. Schematic diagram of the MAPK/RAS signaling pathway.

MAPK/ERK signaling pathway



DISCUSSION

The treatment of HCC has been continuously developed and improved in recent decades, showing a diversified trend. Currently, the existing treatment methods mainly include classical surgical treatment, transarterial chemoembolization, radiofrequency ablation, radiotherapy, molecular targeted drug therapy, immunotherapy, chemotherapy and Chinese herbal medicine, etc., while the treatment concept of HCC has gradually tended to be a holistic treatment mainly based on surgery [1]. However, due to the insidious onset of HCC and the lack of effective early screening means, the diagnosis of HCC often misses the best treatment stage, and the disease is highly heterogeneous and has a high recurrence rate, coupled with the relative insensitivity to radiotherapy and chemotherapy, resulting in a generally poor prognosis for HCC patients, which is largely different from patients expectations [5-7], and the current statistics show that the 5-year survival rate of hepatocellular carcinoma patients is only 12.1%. Analysis of the incidence and mortality rates of liver cancer in the Chinese population over the past 30 years shows that the incidence and mortality rates of liver cancer in the Chinese population are significantly decreasing, but in the next 20 years, the annual number of incidence and deaths of liver cancer in the Chinese population will still exceed 100,000, so HCC will continue to be an important health issue in the near future [8]. A large number of relevant studies have shown that biological processes such as gene mutations, molecular signaling pathways and epigenetic dysregulation are associated with the development of hepatocellular carcinoma, which offers the possibility of explaining cancer development at the genetic level and treating it effectively [9-12].

Kidney cancer is the second most common tumor in the genitourinary system after bladder tumor, and the main pathological type of kidney cancer in China is CCRCC. Surgery is still the main treatment for early to mid-stage kidney cancer. However, like HCC, about 25% of kidney cancers have already developed distant metastases at the time of diagnosis, losing the opportunity for surgical treatment and being naturally insensitive to radiotherapy and chemotherapy, while about 20% of patients were found to have recurrence or metastasis after surgery during follow-up, and the 5-year survival rate of patients with metastatic kidney cancer is less than 10%, with generally very poor prognosis [13,14]. Currently, with the in-depth research on tumors and the discovery of immune checkpoint inhibitor drugs, tumor immunotherapy has become the latest inflection point, and the approved applications of successful cases have greatly increased the confidence of researchers and patients, and medical researchers generally believe that immunotherapy may revolutionize the treatment paradigm and philosophy of cancer [14-17].

Ferroptosis has been found to be closely related to tumors, and the induction of ferroptosis facilitates tumor cell death and inhibits tumor progression, and the induction of ferroptosis process can promote the sensitivity of some drug treatments and radiotherapy sensitivity, which provides new research directions for the treatment of tumors [18,19]. In this study, analysis of ferroptosis gene expression in HCC and CCRCC based on GEO data showed that a large number of ferroptosis genes were expressed in both cancers compared to normal tissues, suggesting that ferroptosis is heavily involved in the metabolic process in both tumors. Further analysis showed that 53 ferroptosis genes were differentially expressed in both two cancers, and enrichment analysis of these intersecting genes revealed that they are mainly involved in the regulation of neuron death and catabolic process, cellular response to external stimulus, scaffold protein binding, wide pore channel activity, protein serine/threonine kinase activity, and other processes. Then the LASSO regression analysis was used to screen for the intersection of the respective signature genes in the two cancers. The results showed that four genes, *CDCA3*, *G6PD*, *NRAS*, and *NDRG1*, were differentially expressed in both HCC and CCRCC, and were common ferroptosis signature genes in both cancers.

Among them, cell division cycle-associated protein 3 (*CDCA3*) is a major regulator of cell mitosis and has been shown to be involved in regulating the proliferation process of many tumor cells, playing an important role in the development of several malignancies [20-23]. Glucose-6-Phosphate Dehydrogenase (*G6PD*) is one of the rate-limiting enzymes that catalyze the pentose phosphate pathway, which prevents cells from oxidative damage by regulating cellular redox homeostasis. *G6PD*-related diseases are more common clinically, mostly due to *G6PD* deficiency, including sericosis, infective hemolysis, and neonatal pathological jaundice [24-26]. In addition, some studies mentioning that *G6PD* expression is associated with proliferation and aggressiveness of colon cancer [27], with higher grade, recurrence and lower survival of hepatocellular carcinoma, after knockdown of *G6PD*, tumor proliferation and metastasis were also inhibited [28]. The neuroblastoma RAS viral oncogene (*NRAS*) is a membrane protein that is located on the surface of the cell membrane and transmits extracellular signals to the nucleus, thus regulating cell proliferation, differentiation and apoptosis. Its mutation rate is high and is common and correlated with patient prognosis mainly in melanoma and colorectal cancer [29]. N-myc downstream regulated 1 (*NDRG1*) is stress-responsive protein involved in hormone responses, cell growth, and differentiation, acting as a tumor Its role in different malignancies is very different, for example, *NDRG1* inhibits proliferation, invasion, and metastasis in nasopharyngeal carcinoma, glioma, pancreatic cancer, etc. [30,31], but promotes proliferation and invasion in bladder cancer, epithelial-mesenchymal transition in esophageal squamous cell carcinoma and stemness features in non-small cell lung cancer [32,33] etc.

Next, we investigated the diagnostic efficacy of the four signature genes in both cancers and their correlation with patient's clinical prognosis. Except for the poor diagnostic efficacy of *G6PD* in CCRCC, all three showed good diagnostic efficacy in both cancers, and in the prognostic analysis the expression of the four signature genes was significantly correlated with the survival prognosis of both cancers, suggesting that all four ferroptosis genes are potential prognostic markers for both cancers. The results of unsupervised cluster analysis based on the expression levels of the four ferroptosis signature genes showed that the two cancers could be classified into two subtypes, which was consistent with the results validated by principal component analysis, and there were statistically significant differences in survival prognosis between the two cancer subtypes. Based on the above findings, we further constructed a risk prediction nomogram model to assess the risk of cancer in patients, and a calibration curve was drawn to verify the accuracy of the predictive power of the line graph. The validation results suggested that the nomogram had good risk prediction power and good net clinical benefit rate and positive detection rate, suggesting the potential of the model for clinical application.

By blocking immune checkpoint recognition, immune checkpoint inhibitors restore the body's specific immune response to tumor cells, prevent immune escape of tumor cells, enhance the anti-tumor ability of immune cells and then kill tumor cells. Targeted therapy based on immune checkpoint research is a new trend in cancer treatment, but the current research on immune checkpoints is still insufficient, and the available targeted drugs are far from meeting the current clinical needs. In this study, we also investigated the correlation between four ferroptosis signature genes and immune checkpoints in two cancers, and the results showed that there were significant correlations between the four signature genes and some immune checkpoints in two cancers, including the classical immune checkpoints *CD274* (PD-1), *PDCD1* (PDL-1), *CTLA4*, etc., suggesting that the expression of signature-based genes can be used as a basis for immune checkpoint therapy. The expression of these genes can predict the immune status and T-cell depletion in the tumor microenvironment to a certain extent, which is of reference

significance for tumor treatment and thus can further predict the prognosis of patients. The correlation between different immune checkpoints was also found to be significant. Currently, single target therapy can no longer meet the clinical demand, and the combination of multiple targets has become a trend, so the study of the correlation between immune checkpoints to clarify the mechanism of action among them is of great reference significance for the development of new targeted drugs.

We also analyzed the relationship between the four signature genes and tumor immune cell infiltration. The results showed that the four signature genes showed significant positive correlation between each of them and most of the immune cells in cancer, while the four signature genes were significantly upregulated in two cancers, suggesting that the expression of the four signature genes influenced the tumor immune microenvironment to some extent and had a certain promotion effect on the immune response of the tumor, which to some extent responded to the tumor immune situation and had some reference significance for the clinical prognosis of patients.

At the end of the study we also explored the signaling pathways involved in four genes, and the results showed that *NRAS* is involved in MAPK/ERK signaling pathway. MAPK/ERK signaling pathway is also found to be involved in the metabolic pathway of hepatocellular carcinoma, thus we further speculate that the upregulation of *NRAS* expression in hepatocellular carcinoma may activate MAPK/ERK signaling pathway to regulate cell proliferation, differentiation and migration, etc.. This is closely related to the prognosis and disease regression of HCC. However, further clinical studies are needed to confirm this conclusion.

There are still many limitations in this study, firstly, the research data used in this study are from different public databases, so the results of this study are affected by the source data, and in addition, the different detection methods among the research data from different sources may lead to deviations among the data, which may affect the results.

CONCLUSION

CDCA3, *NRAS*, and *NDRG1* showed good diagnostic efficacy in HCC, RCC and are potential diagnostic targets for both cancers, and the expression levels of *CDCA3*, *G6PD*, *NRAS*, and *NDRG1* were significantly correlated with the survival of both cancers and are prognostic markers for both cancers. Upregulation of *NRAS* expression may contribute to the pathogenesis and progression of HCC/CCRCC through activation of MAPK/ERK signaling pathway.

DATA AVAILABILITY

The data used in this study were obtained from The Cancer Genome Atlas (TCGA, <https://portal.gdc.cancer.gov/>) database and the GEO (<https://www.ncbi.nlm.nih.gov/geo/>) database, both of which are available in publicly available databases. This study complies with its data use and publication rules.

CONFLICTS OF INTEREST

We declare that there is no conflict of interest regarding the publication of this paper.

FUNDING

No funding support for present study.

AUTHOR'S CONTRIBUTIONS

Xusheng Zhang and Hongcai Zhou contributed equally. Xusheng Zhang, Hongcai Zhou and Bendong Chen participated in the conception and design of the study. Xusheng Zhang and Peng Wei organized the database and statistical analysis. Bendong Chen/Hongcai Zhou/Wei Ma divided the work and participated in the picture drawing. Xusheng Zhang wrote the first draft of the manuscript. Bendong Chen and Hongcai Zhou participated in the revision of the manuscript. All authors read and agreed to the final manuscript and authorship arrangement.

COMPETING INTERESTS

The authors have declared that no competing interest exists.

AVAILABILITY OF DATA

The datasets GSE36961 and GSE32452 in this study were obtained from the GEO (<http://www.ncbi.nlm.nih.gov/geo/>). The MR utilized GWAS data for STAT3 from the GWAS summary data database (GWAS ID: prot-a-2869)

REFERENCES

1. Bureau of medical administration, National Health Commission of the People's Republic of China. Standardization for diagnosis and treatment of hepatocellular carcinoma. *Chinese Journal of Hepatology*. 2022;30:367-388.
2. Grandhi MS, et al. Hepatocellular carcinoma: From diagnosis to treatment. *Surg Oncol*. 2016;25:74-85.
3. Sung H, et al. Global cancer statistics 2020: GLOBOCAN estimates of incidence and mortality worldwide for 36 cancers in 185 countries. *CA-Cancer J Clin*. 2021;71:209-249.
4. Ettrich TJ, et al. Regorafenib. *Recent Results Cancer Res*. 2018;211:45-56.
5. Markham A. Cabozantinib plus nivolumab: A review in advanced renal cell carcinoma. *Target Oncol*. 2022;17:193-201.
6. Yang MH, et al. Somatic mutations of *PREX2* gene in patients with hepatocellular carcinoma. *Sci Rep*. 2019;9:2552.
7. Zeng H, et al. Changing cancer survival in China during 2003-15: A pooled analysis of 17 population-based cancer registries. *Lancet Glob Health*. 2018;6:e555-e567.
8. Julien C, et al. Histological subtypes of hepatocellular carcinoma are related to gene mutations and molecular tumour classification. *J Hepatol*. 2017;67:727-738.
9. Rebouissou S, et al. Advances in molecular classification and precision oncology in hepatocellular carcinoma. *J Hepatol*. 2020;72:215-229.
10. Molina-Sanchez P, et al. Cooperation between distinct cancer driver genes underlies intertumor heterogeneity in hepatocellular carcinoma. *Gastroenterology*. 2020;159:2203-2220.
11. He S, et al. WNT/ β -catenin signaling in the development of liver cancers. *Biomed Pharmacother*. 2020;132:110851.
12. Doehn C. New drugs for metastatic kidney cancer. *Aktuelle Urol*. 2008;39:41-52.
13. Cao X, et al. Real-world clinical outcomes of pazopanib immediately after discontinuation of immunotherapy for advanced renal cell carcinoma. *Clin Genitourin Cancer*. 2020;18:e37-e45.
14. Motzer RJ, et al. Nivolumab plus cabozantinib versus sunitinib in first-line treatment for advanced renal cell carcinoma (CheckMate 9ER): Long-term follow-up results from an open-label, randomised, phase 3 trial. *Lancet Oncol*. 2022;23:888-898.
15. Cavaliere C, et al. Current and emerging treatments for metastatic renal cell carcinoma. *Curr Cancer Drug Targets*. 2018;18:468-479.
16. Chen X, et al. Broadening horizons: The role of ferroptosis in cancer. *Nat Rev Clin Oncol*. 2021;18:280-296.
17. Qian W, et al. *CDCA3* mediates p21-dependent proliferation by regulating *E2F1* expression in colorectal cancer. *Int J Oncol*. 2018;53:2021-2033.
18. Phan NN, et al. Distinct expression of *CDCA3*, *CDCA5*, and *CDCA8* leads to shorter relapse free survival in breast cancer patient. *Oncotarget*. 2018;9:6977-6992.
19. Zhang Y, et al. *CDCA3* is a potential prognostic marker that promotes cell proliferation in gastric cancer. *Oncol Rep*. 2019;41:2471-2481.
20. Shang X, et al. Update in the genetics of thalassemia: What clinicians need to know. *Best Pract Res Clin Obstet Gynaecol*. 2017;39:3-15.
21. Sagiv E, et al. Glucose-6-phosphate-dehydrogenase deficient red blood cell units are associated with decreased post transfusion red blood cell survival in children with sickle cell disease. *Am J Hematol*. 2018;93:630-634.
22. Commons RJ, et al. The haematological consequences of *Plasmodium vivax* malaria after chloroquine treatment with and without primaquine: A worldwide antimalarial resistance network systematic review and individual patient data meta-analysis. *BMC Med*. 2019;17:151.
23. Zhang X, et al. PAK4 regulates G6PD activity by p53 degradation involving colon cancer cell growth. *Cell Death Dis*. 2017;8:e2820.
24. Barajas JM, et al. The role of miR-122 in the dysregulation of glucose-6-phosphate dehydrogenase (G6PD) expression in hepatocellular cancer. *Sci Rep*. 2018;8:9105.
25. Mele L, et al. A new inhibitor of glucose-6-phosphate dehydrogenase blocks pentose phosphate pathway and suppresses malignant proliferation and metastasis *in vivo*. *Cell Death Dis*. 2018;9:572.
26. Funck-Brentano E, et al. Increase in *NRAS* mutant allele percentage during metastatic melanoma progression. *Exp Dermatol*. 2016;25:472-474.
27. Schirripa M, et al. Role of *NRAS* mutations as prognostic and predictive markers in metastatic colorectal cancer. *Int J Cancer*. 2015;136:83-90.
28. Ma W, et al. Overexpression of N-myc downstream-regulated gene 1 inhibits human glioma proliferation and invasion *via* phosphoinositide 3-kinase/AKT pathways. *Mol Med Rep*. 2015;12:1050-1058.

29. Cen G, et al. Downregulation of the N-myc downstream regulated gene 1 is related to enhanced proliferation, invasion and migration of pancreatic cancer. *Oncol Rep.* 2017;37:1189-1195.
30. Ai R, et al. *NDRG1* overexpression promotes the progression of esophageal squamous cell carcinoma through modulating Wnt signaling pathway. *Cancer Biol Ther.* 2016;17:943-954.
31. Chang X, et al. *NDRG1* controls gastric cancer migration and invasion through regulating MMP-9. *Pathol Oncol Res.* 2016;22:789-796.
32. Wang Y, et al. N-myc downstream regulated gene 1 (*NDRG1*) promotes the stem-like properties of lung cancer cells through stabilized c-Myc. *Cancer Lett.* 2017;401:53-62.
33. Li A, et al. Upregulation of *NDRG1* predicts poor outcome and facilitates disease progression by influencing the EMT process in bladder cancer. *Sci Rep.* 2019;9:5166.